Advances in X-Ray Analysis, Vol. 31

BNL--40374

DE88 002120

X-Ray Microscopy Using Collimated and Focussed Synchrotron Radiation

K. W. Jones, W. M. Kwiatek, B. M. Gordon, A. L. Hanson, J. G. Pounds
Brookhaven National Laboratory, Upton, New York 11973

M. L. Rivers, S. R. Sutton
University of Chicago, Chicago, Illinois 60637

A. C. Thompson, J. H. Underwood, R. D. Giauque, and Y. Wu
Lawrence Berkeley Laboratory, Berkeley, California 94720

Presented at

36th Annual Denver X-Ray Conference

Denver, Colorado

August 3-7, 1987

X-RAY MICROSCOPY USING COLLIMATED AND FOCUSSED SYNCHROTRON RADIATION*

K. W. Jones, W. M. Kwiatek, B. M. Gordon, A. L. Hanson, J. G. Pounds
Brookhaven National Laboratory
Upton, NY 11973

M. L. Rivers, S. R. Sutton
University of Chicago
Chicago, IL 60637

A. C. Thompson, J. H. Underwood, R. D. Giauque, Y. Wu
Lawrence Berkeley Laboratory
Berkeley, California 94720

INTRODUCTION

X-ray microscopy is a field that has developed rapidly in recent years. Two different approaches have been used. Zone plates have been employed to produce focussed beams with sizes as low as 0.07 μm for x-ray energies below 1 keV.[1] Images of biological materials and elemental maps for major and minor low Z have been produced using above and below absorption edge differences.[2] At higher energies collimators and focussing mirrors have been used to make small diameter beams for excitation of characteristic K- or L-x rays of all elements in the periodic table.

The practicality of a single instrument combining all the features of these two approaches is unclear. The use of high-energy x rays for x-ray microscopy has intrinsic value for characterization of thick samples and determination of trace amounts of most elements. A summary of work done on the X-26 beam line at the National Synchrotron Light Source (NSLS) with collimated and focussed x rays with energies above 4 keV is given here.

*Work supported in part by Processes and Techniques Branches, Division of Chemical Sciences, Office of Basic Energy Sciences, US Department of Energy, under Contract No. DE-AC02-76CH00016; Director's Office of Energy Research, Office of Health and Environmental Research, US Department of Energy Contract No. DE-AC03-76SF00098; applications to biomedical problems by the National Institutes of Health as a Biotechnology Research Resource under Grant No. P41RR01838; applications in geochemistry by National Science Foundation Grant No. EAR-8618346; and applications in cosmochemistry by NASA Grant No. NAG 9-106.

The difficulties in the mapping of trace elements at the concentration level of 1 part-per-million (ppm) for a sample volume of 10 μm × 10 μm × 10 μm (10^{-9} cm^3) using detection of characteristic x rays is quite comparable to that involved in measuring the transmission of a 0.1 μm × 0.1 μm beam through a sample thickness of about 1-10 μm represented by a biological cell. In the former case there are only about 10^7 atoms present to produce a signal if it is assumed that there is 1 ppm of zinc present in a matrix with density of 1 g/cm^3. In the latter case the sample volume is about .01 to .1 μm^3 and the number of atoms that produce a signal for imaging density differences is about 10^5, assuming a carbon matrix with density of 1 g/cm^3. The first determination is made possible by having a large number of incident photons, while the second relies on using a large number of target atoms to produce changes in the transmission of a smaller beam. The challenges are different, but both types of microscopy require the utmost of existing experimental capabilities.

A versatile high-energy x-ray fluorescence microscope system is now in operation on the X-26 beam line at the Brookhaven National Synchrotron Light Source. Two types of instruments have been used for experiments. One is based on the use of collimated white radiation, the second adds a Kirkpatrick-Baez[3] system with multilayer-coated mirrors to produce a focussed beam of 10-kev photons. The two systems are complementary in attributes and, if considered together, form a versatile x-ray microscope system for trace element determinations. System parameters are described, and typical values for minimum detection limits for the two modes of operation are presented here.

CHARACTERISTICS OF THE NSLS X-RAY SOURCE

The work presented here was done with the white beam generated by a bending magnet source at the NSLS. The x-ray beam used in the x-ray microscopes (XRM) was defined with a variable width aperture located 20 m from the x-ray source point at the electron orbit in the storage ring. The x-ray spectrum can be described adequately by a curve showing x-ray flux as a function of x-ray energy. The high source brilliance (emission/mm^2/$mrad^2$/mA) is important since it ensures that there is maximum photon polarization at the sample and hence maximum reduction of scattered radiation at 90° to the incident beam. Background radiation is thereby minimized. In the future, a focussing mirror will be added to the system to take additional advantage of the high brilliance of the NSLS. The x-ray flux produced by the NSLS at the X-26 beam line is shown in Figure 1 and the integrated energy distribution above a photon energy, E, is shown as a function of E in Figure 2.

Typical average electron currents in the storage ring were about 100 mA. Peak stored currents at injection were as high as 220 mA. The actual x-ray beam flux and energy at the sample are dependent on the system that follows the collimator at 20 m as discussed below.

COLLIMATED X-RAY MICROSCOPE

The collimated XRM (CXRM) used only the variable size rectangular slits at 20 m to define the size of the x-ray beam. This simple technique was used to form beams with sizes down to around 20 μm.

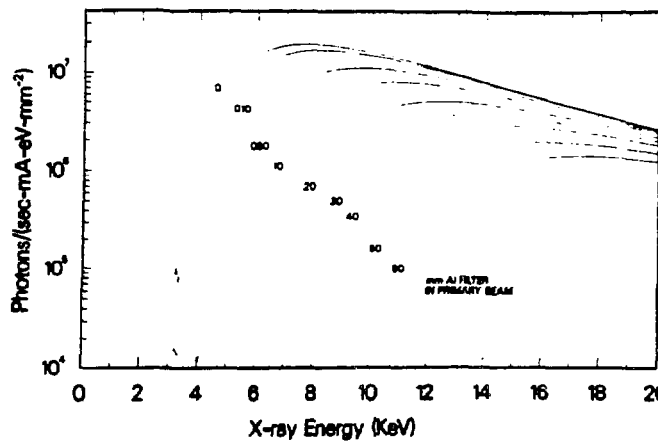

Figure 1. Energy distribution of the photons used for the CXRM and the FXRM in units of photons/(s-mA-eV-mm^2). Effects of beryllium windows in the beam line and various thicknesses of aluminum filters in the beam are shown by the different curves.

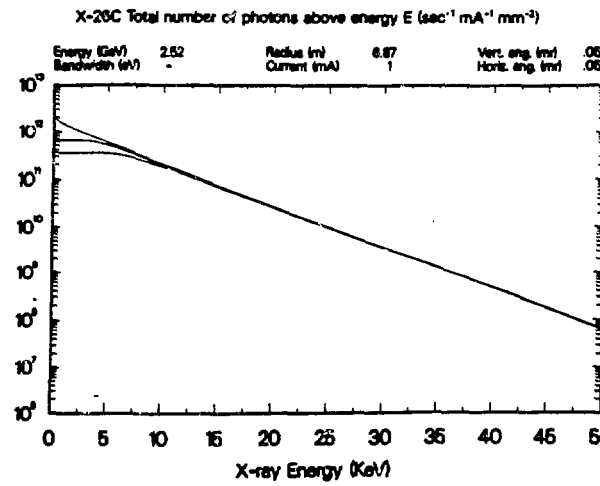

Figure 2. Integrated number of photons with an energy above a photon energy, E, shown as a function of E. The numbers are given in units of photon/(s-mA-mm^2).

The beam divergence after emerging from the collimator depends on the x-ray source size at the electron orbit. The NSLS arc magnet source is about 400 μm (Horizontal) x 100 μm (Vertical) for one standard deviation from the beam maximum. Thus the intrinsic horizontal angular spread at the XRM is about 2×10^{-5} rad. This divergence is sufficiently small that it is not critically necessary to place the sample stage close to the defining slits. Room is thus available for an ion chamber between the slits and specimen to monitor photon flux and for an optical microscope to use for sample placement relative to the beam. In our instrument the collimator to sample distance was 40 cm so that the intrinsic minimum spatial resolution was around 16 μm (2 sigma width).

The beam size was investigated by doing one-dimensional scans of a gold replica of an electron microscopy grid. It was found that it was indeed possible to obtain resolutions of about 20 μm, in agreement with the estimate based on the source size and resulting angular divergence. If better resolution is needed, it can be obtained by using a defining slit located closer to the sample position. The photon flux is sufficiently high that it is feasible to work with a beam size of 10 μm x 10 μm or less with acceptable values of sensitivities.

The samples were mounted on a stepper-motor-driven x,y,z,θ stage that could be used to position the sample to an accuracy and reproducibility of 1 μm or less. The stage was program controlled from a Digital Equipment Corporation MicroVAX II computer system.

Data acquisition was handled from a Nuclear Data Corporation ND 9900 pulse height analysis system. This system is based on the use of the MicroVAX II computer and operating system so that the data acquisition and system control programs could be conveniently integrated into a single entity. The data acquisition could be handled in several different ways with sequential storage of complete x-ray spectra from a Si(Li) x-ray detector at different points, or by a raster-type map with storage of background corrected points for selected elements of interest at each PIXEL.

The x-ray detector that was used had an energy resolution of about 150 eV at 5.9 keV at low counting rates. The sensitive area was 30 mm^2, but generally a 3-mm diameter silver aperture with a thickness of 0.3 mm was used in an effort to reduce the effects of Compton scattering and poor detection efficiency near the silicon crystal edges. The beam spot to detector distance was 4 cm. This detector arrangement was suitable for general use, but was not optimized for best performance in making maps or in working with the smallest possible collimator apertures.

The collimated XRM used the continuous spectrum of x rays from the bending magnet source. The spectrum was modified by the use of three beryllium windows in the beam line with a total thickness of 508 μm to separate the ultrahigh vacuum conditions existing in the storage ring and beam pipe from the XRM which was operated in air at atmospheric pressure. The beam was further modified by the thin polyimide windows and helium gas contained in the ion chamber and the final section of beam pipe; however, these effects were small compared with the absorption by the ion chamber-to-specimen air path.

Additional attenuators were used in the primary beam in order to optimize sensitivity for given elements. Thin aluminum foils were generally employed for this purpose. Generally, a foil thickness was

chosen to attenuate the beam at energies below the threshold for production of some particular element of interest. The background of scattered x rays underneath the peak of interest was reduced with the filter, but, of course, the number of x rays at energies above the absorption edge was also reduced. The background reduction was the larger effect.

Attenuators were also used on the x-ray detector to reduce the counting rate from abundant elements that produced x rays at energies lower than those from the elements of interest. Several hundred micrometer thicknesses of polyimide foils were usually sufficient.

The total flux of x rays delivered to the sample is estimated from the calculations shown in Figure 1 to be about 3×10^7 photons/sec/μm^2 at 70 mA when integrated over all photon energies. This theoretical value is in agreement with an experimental determination based on the monitor ion chamber currents and with a calculation of the number of fluorescent x rays produced by irradiation of a sample with a known number of target atoms. Values determined from Figure 1 are overestimates since the actual fluxes will be reduced by fluctuations in the vertical electron beam position. Since beam instabilities of up to 1 mm were observed during routine NSLS operation, this could be a significant effect.

FOCUSSED X-RAY MICROSCOPE

The focussed XRM (FXRM)[4] utilizes a Kirkpatrick-Baez mirror geometry. The focussing mirrors intercepted photons from the source that passed through an aperture of 500 μm × 500 μm normal to the beam 20 m from the source. The variable collimators used in the CXRM were used to restrict the incident x rays to that size and prevent passage of x rays that could not be accepted by the mirrors. The apparatus used after the mirrors is identical to the CXRM described above.

The Kirkpatrick-Baez system comprises two spherical focussing mirrors, the first focussing in the horizontal plane and, the second in the vertical plane. The mirrors were coated with synthetic multilayers so that the incident white beam was made monochromatic in addition to being focussed. The properties of the multilayers were adjusted so that both horizontal and vertical mirrors brought the beam to a focus at the same point about 5 cm from the second mirror. Spherical mirrors made of quartz with a radius of curvature of 600 cm and a surface roughness of about .3 nm were used. The multilayers were W-C with a 2d spacing of 8.7 nm for the first mirror and 6.3 nm for the second. The number of multilayer pairs used was 100 for both mirrors which was sufficient to give high efficiency for transmission of 10 keV x rays. The bandpass for the system at 10 keV was about 1 keV.

The image size was optimized by adjusting the size of the fluorescent image produced in a thin ruby crystal. The mirror angles and spacing could be remotely adjusted using computer-controlled stepper motors while viewing the image size and the energy of the radiation scattered from the ruby as measured in the Si(Li) detector positioned at 90° from the incident beam. The beam size was measured on a transmission electron microscope grid to be less than 10 μm × 10 μm.

The photon flux was measured using an ion chamber and by detection of fluorescent radiation as was done for the CXRM case. A value of 2 × 10^9 photons/s was found at a stored electron current of 100 mA. This number should correspond to the number of photons transmitted by the initial collimator with an area of 0.25 mm^2. The number of photons incident on the aperture can be calculated from the curves shown in Figures 1 and 2. A value of .6 × 10^{11} photons/s is found at a stored current of 100 mA. Comparison of the two photon current values the shows that the overall efficiency of the Kirkpatrick-Baez mirror system for transmission of the 10 keV x rays is about .2%. (This does not correspond to a measurement of the multilayer transmission, but to the efficiency of the entire FXRM system.)

EXPERIMENTAL RESULTS AND DISCUSSION

The performance of the two XRMs was investigated by measuring the minimum detection limits (MDLs) for fluorescent x-ray peaks produced by a series of standard reference samples. One useful reference sample was produced by adding a number of elements to gelatin at a concentration level of 10 ppm by wet weight. Thin sections were produced by standard microtome techniques. Fluorescent spectra observed using the CXRM and the FXRM are shown in Figures 3 and 4.

The differences in the spectra show that the CXRM using white radiation is valuable in situations where extended elemental sensitivity is required and for analysis of heavy elements with absorption edges above the energy range conveniently reached by multilayer mirrors. The MDLs achieved in each case can be evaluated from the number of counts in the observed peaks. The results are shown in Table 1 where the values are normalized to 60-s runs at a beam size of 10 μm × 10 μm. The MDLs obtained with the FXRM are better than for the FXRM although the differences are possibly tilted to the FXRM at the energies close to the 10-keV beam energy. This is because the CXRM used a somewhat lower energy beam cut-off that resulted in higher backgrounds above about 5 keV.

Table 1. Minimum Detection Limits

	V	Fe	Zn	Br	Sr		V	Fe	Zn	Br	Sr
			(fg)						(pg)		
Thin Gelatin Standard						Thick IAEA H-5 Animal Bone Standard					
F	8	2.2	3.1	—	—	F	—	1.6	.31	—	—
C	41	9.6	36.6	—	—	C	—	32.0	8.3	2.8	.026

F = Focussed, 10 keV photon energy
C = Collimated, white light photon energy spectrum
t = 60 s
A = 10 × 10 μm^2
Ring Current = 67 mA

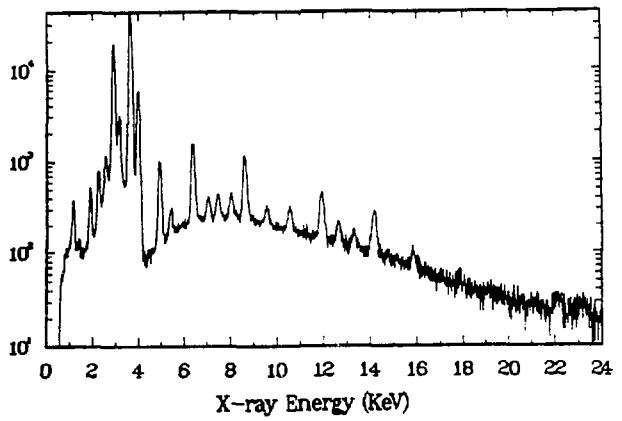

Figure 3. Spectrum for fluorescent x rays from a 20-μm thick gelatin standard obtained with the CXRM. The run was done with 75 μm x 75 μm beam size, 64 mA ring current, and a live time of 200 s. A 25.4-μm aluminum filter was used on the primary beam and a 7.6-μm polyimide filter was used on the detector.

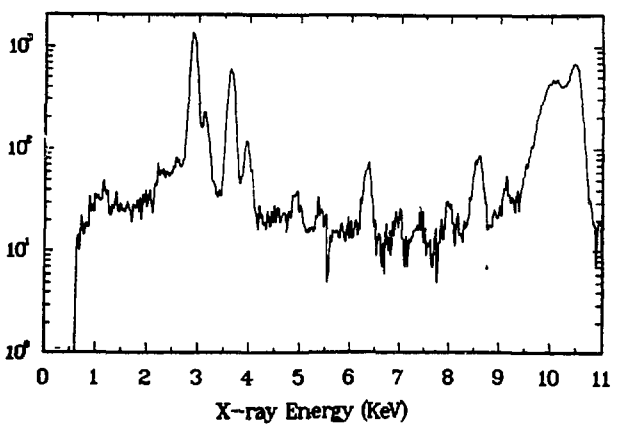

Figure 4. Spectrum for fluorescent x rays from the 20-μm thick gelatin standard used to obtain the data shown in Figure 2, but taken with the FXRM. The beam size was about 10 μm x 10 μm, the live time 300 s, and the ring current 69 mA. No filters were used.

The two different samples listed in Table 1 were taken to represent extremes in thickness. The results for the gelatin sample can be largely explained by differences in the backgrounds observed with the Si(Li) detector. The MDLs should differ by a factor of 4-5 in favor of the FXRM without taking into account the variations in energy distribution of the photon beams in the two cases. The relative values calculated for the bone sample are more complex since the amount of target atom used effectively in the measurement must be integrated over the sample thickness. The backgrounds for the white beam are, however, a bigger factor than for the case of a thin sample which will also explain most of the difference in the detection sensitivity.

The gains in photon flux obtained from focussing the beam are counterbalanced to a certain extent by the use of the white beam in the CXRM. The measured values for the numbers of photons per second were shown to be roughly equivalent. The MDL results are affected by the differences in the energy distributions and backgrounds. The CXRM is the more flexible and simpler of the two since it can be used to make measurements on all elements with absorption edges up to say 80 or 90 keV albeit with sharply increasing values for the MDLs. The FXRM has advantages for applications where the ultimate in spatial resolution is desired, below about 10 μm resolution, and for the best value of MDL for a particular element.

Elemental maps have been made with both microscopes. Time needed for a map depends on the size of the area scanned and the concentration of the elements of interest. Typically, the map might contain about 2500 pixels. If data acquisition, analysis, and stage motion take a total of a few seconds per pixel, it can be seen that the time for a single map will be around several hours.

Figure 5 shows a map made of the gallium distribution in a 20-μm section of fetal rat bone obtained with the CXRM.[5] A photomicrograph is also included to show the relationship between the gallium distribution and the biological features of the bone. The map was made with a pixel size of 40 μm x 40 μm. This was chosen to be consistent with the size of the important biological features and to allow coverage of a comparatively large area of sample in a reasonable time. Comparison of the gallium map with the photomicrograph shows that the gallium is concentrated in the region of the bone that contains calcium and that it is most abundant in the region of the growth plate.

This map was made as part of an initial investigation of the pharmaco-dynamics involved in the use of gallium nitrate in the treatment of hypocalcemia, a bone disorder occurring in types of bone cancer. The gallium nitrate is found to stop calcium loss and is coming into general use as a therapeutic agent. It is possible that it will have wider use to treat other bone diseases such as osteoporosis. Maps, such as the one displayed above, will be used to determine the rate of gallium absorption in rats so that ideas can be gained on how to treat human patients in an optimum way.

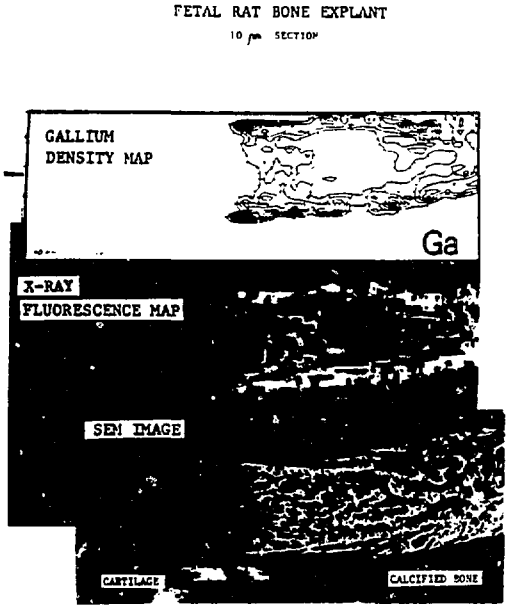

Figure 5. Composite figure showing the distribution of gallium in foetal rat bone taken with the CXRM. The lowest picture is a photomicrograph of the 10-μm section of foetal rat bone showing the region scanned. The top two displays show the gallium distribution in terms of a contour plot (top) and a density plot (center) where the light regions indicate the highest concentration levels. The pixel size in the map is 40 μm × 40 μm. The results show that the gallium is concentrated in the region of calcified bone.

SUMMARY AND CONCLUSIONS

A comparison has been made of the performance of a CXRM and a FXRM, and examples of their use have been given. The CXRM has extended energy sensitivity and is simple to construct and operate. It is able to produce beam sizes which are close to those achieved by the FXRM, but the sensitivity attained is not as good. Hence, the CXRM is an excellent choice for work with photons above 10 keV and for survey experiments that need as wide an energy range as possible. The FXRM seems superior for work when both the best spatial resolution and MDLs are sought.

There are several parameters that enter into the performance of each type of XRM. The work that we describe here is only the first in a series of experiments that will examine how the performance of each XRM can be improved. Use of higher photon fluxes achieved by use of a focussing mirror prior to the XRM focussing system should improve the MDLs that can be attained by one to two orders of magnitude. This will make it possible to detect of the order of 10^4 to 10^6 atoms.[6] The higher flux should also ultimately lead to shorter map times after provision is made for faster scan rates and data handling.

Both the high-energy CXRM and FXRM have been shown to operate successfully at this time. In the future, improvements to the sensitivity and to the spatial resolution should be feasible so that operation around the 1-μm region can be expected. At that point it will be interesting to consider the comparative advantages of the types of XRM considered here and the high-spatial resolution types that are based on the use of zone plates.

REFERENCES

1. C. Jacobsen, J. M. Kenney, J. Kirz, I. McNulty, R. J. Rosser, F. Cinotti, H. Rarback, and D. Shu, Microanalysis with a soft x-ray scanning microprobe, Ann. N.Y. Acad. Sci., 483:463 (1986); J. Kirz and D. Sayre, Soft x-ray microscopy, Nucl. Instrum. Methods, in press.
2. J. M. Kennedy, C. Jacobsen, J. Kirz, H. Rarback, F. Cinotti, W. Thomlinson, R. Rosser, and G. Schidlovsky, Absorption microanalysis with a scanning soft x-ray microscope: mapping the distribution of calcium in bone, J. Microscopy 138(3):321 (1985).
3. P. Kirkpatrick and A. V. Baez, J. Opt. Soc. Amer. 38:766 (1948).
4. A. C. Thompson, J. H. Underwood, Y. Wu, R. Giauque, K. Jones, and M. Rivers, Elemental measurements of biological and geological samples using an x-ray microprobe, Nucl. Instrum. Methods, in press.
5. R. Bockman, M. Repo, R. Warrell, J. G. Pounds, W. M. Kwiatek, G. J. Long, G. Schidlovsky, and K. W. Jones, X-ray microscopy studies on the pharmaco-dynamics of therapeutic gallium in rat bones, in: "Proc. The International Symposium on X-Ray Microscopy, Upton, NY, August 1987," to be published.
6. B. M. Gordon and K. W. Jones, Design criteria and sensitivity calculations for multielemental trace analysis at the NSLS x-ray microprobe, Nucl. Instrum. Methods B10/11:293 (1985).